THE JOURNAL OF PHYSICAL CHEMISTRY B

Article

pubs.acs.org/JPCB

Glass Transition and Relaxation Processes of Nanocomposite Polymer Electrolytes

Benson K. Money,*[,†] K. Hariharan,[‡] and Jan Swenson[†]

[†]Department of Applied Physics, Chalmers University of Technology, SE-412 96 Göteberg, Sweden

[‡]Department of Physics, Indian Institute of Technology Madras, Chennai-600036, India

ABSTRACT: This study focus on the effect of δ-Al_2O_3 nanofillers on the dc-conductivity, glass transition, and dielectric relaxations in the polymer electrolyte $(PEO)_4$:$LiClO_4$. The results show that there are three dielectric relaxation processes, α, β, and γ, in the systems, although the structural α-relaxation is hidden in the strong conductivity contribution and could therefore not be directly observed. However, by comparing an enhanced dc-conductivity, by approximately 2 orders of magnitude with 4 wt % δ-Al_2O_3 added, with a decrease in calorimetric glass transition temperature, we are able to conclude that the dc-conductivity is directly coupled to the hidden α-relaxation, even in the presence of nanofillers (at least in the case of δ-Al_2O_3 nanofillers at concentrations up to 4 wt %). This filler induced speeding up of the segmental polymer dynamics, i.e., the α-relaxation, can be explained by the nonattractive nature of the polymer−filler interactions, which enhance the "free volume" and mobility of polymer segments in the vicinity of filler surfaces.

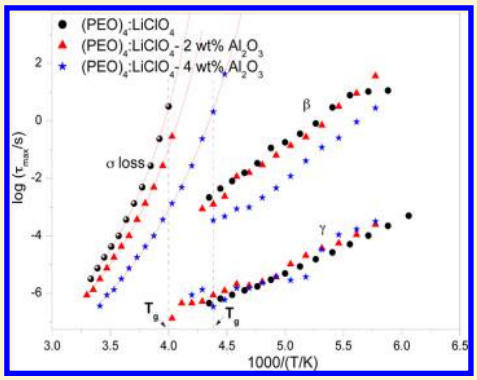

1. INTRODUCTION

Solid polymer electrolytes (SPE) have received considerable attention for several decades due to their technological importance in a wide variety of devices such as batteries, fuel cells, supercapacitors, hybrid power sources, sensors, etc. These SPEs are based on polymers, rather than liquids, which provide major advantages, such as leak proof, high energy density, lightweight, good mechanical stability, weak flammability, and low dendrite formation. The basic requirements of the polymer electrolytes to be used in devices are high conductivity at room temperature, low electronic conductivity, good mechanical properties, and thermal, chemical, and electrochemical stability. However, most polymer electrolytes, such as poly(ethylene oxide) (PEO) based electrolytes, exhibit very poor ionic conductivity (up to about 10^{-5} S cm^{-1} at 370 K), which is a serious barrier in potential technological applications.[1] PEO-based electrolytes are, in general, semicrystalline in nature and composed of spherulites with thin amorphous layers between them. The ion migration is believed to occur predominantly in the amorphous rich phase, where the transport properties (ionic conductivity, mechanical relaxations, diffusion, spin relaxation, etc.) are directly associated with the large-scale segmental motion of the polymer. These SPE systems are often considered to be coupled systems (i.e., the ionic diffusion is a combination of structural relaxation processes) as well as by the independent movement of ions.[2] However, the semicrystalline nature of PEO-based electrolytes hinders the ionic conductivity and suppresses the dielectric relaxations.

The addition of ultrafine inert fillers, like Al_2O_3, $BaTiO_3$, ZrO_2, MgO, CeO_2, etc., in polymer electrolytes has attracted considerable research efforts, in order to reduce crystallinity and enhance the transport properties of polymer electrolytes.[3−7] This new class of SPEs, i.e., composite polymer electrolytes (CPEs), exhibits improved physicochemical properties. Studies have shown that the improved properties are very much dependent on the size, concentration, and chemical nature of the surface groups of the fillers and the filler−chain interactions. These fillers also tend to affect the ion-pairing and ion-clustering in polymer electrolytes. Previous studies have shown that the addition of nanosize α-Al_2O_3 particles to the PEO:$LiBF_4$ system enhanced the conductivity by 1 order of magnitude as compared to the addition of micrometer-sized particles.[8] Another study[9] has shown that the addition of ferroelectric $BaTiO_3$ particles of micrometer size enhance the ionic conductivity of the PEO:$LiClO_4$ system. Several qualitative explanations, like Lewis acid−base interactions between the ions and the fillers, thereby improving the dissociation of ion clusters and uncomplexed salt, and surface activity of the filler particles and creation of static pathways for ionic motion by decoupling the diffusion and the relaxation of the conducting species, are supported by various studies.[4,10,11] The present study is mainly focused on how the ionic conductivity, glass transition temperature, and relaxation processes are altered by the introduction of nanofillers to a PEO-based polymer−salt complex system. The presence of three clearly observable relaxation processes, i.e., α-, β-, and γ-relaxations, in PEO have been found in previous studies.[12−14] The segmental motions of the amorphous parts of the main

Received: April 16, 2012
Revised: June 9, 2012
Published: June 11, 2012

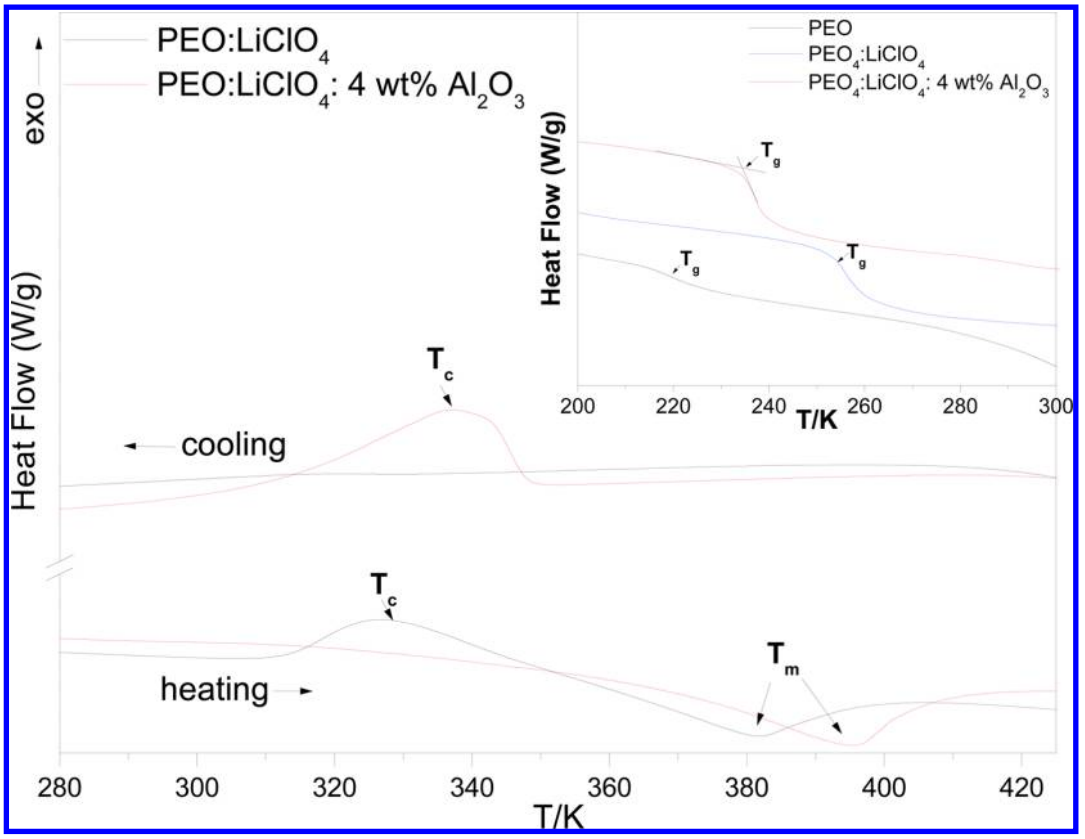

Figure 1. DSC plots of $(PEO)_4$:$LiClO_4$:*x* wt % δ-Al_2O_3 (*x* = 0 and 4). Inset: Glass transition of PEO and $(PEO)_4$:$LiClO_4$:*x* wt % δ-Al_2O_3 (*x* = 0 and 4).

polymer chains of PEO are associated with the α-relaxation, whereas the β-relaxation is attributed to more local segmental motions of polymer chains in also amorphous regions and therefore mainly affected by the crystallinity content of the polymer. The γ-relaxation peak may be associated with the local intramolecular twisting motion of ethylene ($-CH_2-CH_2-$) parts or local motions of the chain ends of the polymer.[14,15]

Dielectric spectroscopy is a suitable experimental technique to probe these relaxation processes, since it often reveals more details of the various relaxation processes than, for instance, the relatively broader features observed in dynamic mechanical spectroscopy and Brillouin scattering. Moreover, the generally broad frequency range of dielectric measurements makes it a particularly versatile method to study slow dynamic processes in polymers and supercooled liquids over broad temperature ranges. In this paper, we report a detailed dielectric spectroscopy study of the ionic conduction and relaxations in the $(PEO)_4$:$LiClO_4$ system with δ-Al_2O_3 nanofillers (~13 nm). The ionic transport of the PEO:$LiClO_4$ system has been well studied,[16,17] but the studies related to the dielectric relaxations in the system and the influence of nanofillers on these dielectric relaxations have drawn less attention. Dielectric studies of such systems can provide deeper insight regarding the ion dynamics, segmental relaxations, and conductivity relaxation, as well as the changes of the dynamical processes in the presence of fillers.

2. EXPERIMENTAL TECHNIQUES

The polymer electrolyte samples were prepared by mixing appropriate quantities of PEO ($M_w = 5 \times 10^5$) and $LiClO_4$ salt in acetonitrile solution. This solution was stirred at room temperature for approximately 24 h. Highly pure, fumed δ-Al_2O_3 (size ~13 nm) fillers were added to the polymer–salt solution to prepare composite polymer electrolytes, i.e., $(PEO)_4$:$LiClO_4$ with 2 and 4 wt % fillers. The composite polymer solutions were stirred continuously until the mixtures appeared to be homogeneous. The solutions were later poured on PTFE Petri dishes and vacuum-dried at 323 K for 48 h to remove all the traces of solvent. In that way, free-standing thin polymer electrolyte films were obtained. The thicknesses of these polymer films were measured in micrometers, giving values of around 100–150 μm.

For thermal characterization, DSC measurements were carried out on a piece of each polymer sample, encapsulated in a hermatic aluminum pan, using a TA Instruments Q1000 DSC. The measurements were carried out from 170 to 430 K with a heating rate of 10 K min^{-1}, under nitrogen atmosphere.

Dielectric measurements were performed with the Novocontrol GmBH Broadband Dielectric spectrometer system with Quatro Cryosystem temperature control unit. Polymer film samples were placed between two gold plated electrodes, and the impedance measurements were performed in the frequency and temperature ranges 10^{-2}–10^7 Hz and 135–365 K, respectively.

3. RESULTS AND DISCUSSION

3.1. Thermal Characterization. The DSC curves, during heating and cooling cycles, of $(PEO)_4$:$LiClO_4$ and $(PEO)_4$:$LiClO_4$ with 4 wt % δ-Al_2O_3 are shown in Figure 1.

The melting temperature of pure PEO is around 338 K. The DSC plot, during the cooling cycle of the polymer electrolyte, $(PEO)_4$:$LiClO_4$, does not show any phase transition in the measured temperature range. However, for $(PEO)_4$:$LiClO_4$

dx.doi.org/10.1021/jp3036499 | J. Phys. Chem. B 2012, 116, 7762–7770

with 4 wt % δ-Al_2O_3, i.e., in the presence of fillers, an exothermic crystallization peak is observed around 335 K. These nanofillers seem to act as multiple nucleation sites for the rapid growth of poorly developed spherulites.[18,19] In the heating cycle, the DSC curve of $(PEO)_4$:$LiClO_4$ exhibits an exothermic crystallization peak at 326 K and an endothermic melting peak at 380 K.[20,21] However, $(PEO)_4$:$LiClO_4$ with fillers exhibited only an endothermic peak at 395 K, corresponding to the melting of the partially crystallized composite electrolyte. The inset of Figure 1 shows the glass transition of the polymer samples. The glass transition temperature (T_g) of pure PEO is located around 215 K. The polymer−salt complex $(PEO)_4$:$LiClO_4$ exhibited a higher T_g around 252 K. The increase in T_g, in the presence of Li^+ salt, can be attributed to a reduction in flexibility of the polymer chains due to the interaction between the ether oxygens of the polymer chains and the Li^+ ions. This also confirms the complexation of the polymer and the salt. Furthermore, it is observed that T_g decreases with increasing filler content (to ∼230 K with 4 wt % δ-Al_2O_3). Previous experimental and theoretical studies of CPE have indicated that, in the presence of fillers, the increase or decrease in T_g depends on how the surface interactions of the fillers affect the dynamics of polymers within an interfacial layer near fillers surfaces,[22−24] i.e., a slowing down (increased T_g) or an acceleration of dynamics (decreased T_g) when the polymer−filler interactions are attractive or repulsive, respectively. Thus, our results indicate that the interaction at the filler−polymer interface may be repulsive in nature and the structural (α) relaxation of the polymer chains speeds up with increasing filler concentration, at least at temperatures around the glass transition temperature.

3.2. Frequency Dependence of the Ionic Conductivity.

Parts a and b of Figure 2 show the real part of the frequency dependent conductivity at different temperatures for $(PEO)_4$:$LiClO_4$:x wt % δ-Al_2O_3 with x = 0 and 4, respectively. The frequency dependence of the conductivity shows three different regions associated with different phenomena: (i) low frequency polarization effects, (ii) a frequency independent dc-conductivity region, and (iii) a high frequency dispersion region. As the temperature increases, the conductivity increases and the dispersion region shifts toward higher frequencies. The crossover from the frequency independent region to the dispersive region indicates the onset of the conductivity relaxation phenomena. The real part of the conductivity, $\sigma'(f)$, can be expressed in terms of the dc-conductivity, σ_{dc}, and a characteristic frequency, f_c, using the Almond−West relation[25]

$$\sigma'(f) = \sigma_{dc}[1 + (f/f_c)^n] \quad (1)$$

where σ_{dc} is the dc-conductivity, f is the frequency, and n is the power-law exponent, with $0 \le n \le 1$. The filled symbols in Figure 2 mark the onset frequency of dispersion, f_c, defined via $\sigma'(f_c) = 2\sigma_{dc}$. This characteristic frequency, f_c, is the crossover frequency from the frequency independent region to the dispersive conductivity region at $f > f_c$. Studies have shown that the crossover frequency, f_c, in the Almond−West model represents a very good approximation of the hopping rate, f_H, associated with the Nernst−Einstein relation, i.e., $f_c \sim f_H$.[26−28] The dc-conductivity, σ_{dc}, and the ion hopping frequency, f_H, were obtained by fitting the real part of the complex conductivity, $\sigma'(f)$, to the above Almond−West relation, for $(PEO)_4$:$LiClO_4$ and $(PEO)_4$:$LiClO_4$ with 4 wt % Al_2O_3.

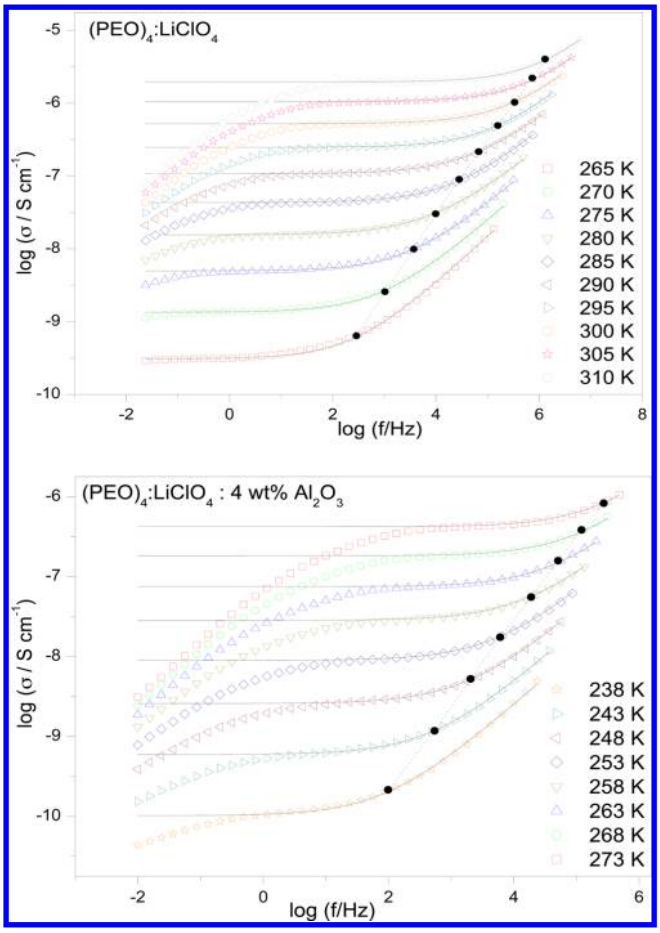

Figure 2. Frequency dependent conductivity plots of (a) $(PEO)_4$:$LiClO_4$ and (b) $(PEO)_4$:$LiClO_4$ with 4 wt % δ-Al_2O_3.

By estimating the "hopping rates" of mobile ions, f_H, the concentration of mobile Li^+ ions can be determined from the Nernst−Einstein relation

$$\sigma_{dc} = en_c\mu = \frac{n_c e^2 \gamma \lambda^2}{k_B T} H_R \omega_H \quad (2)$$

where n_c is the concentration of mobile charge carriers, μ is their mobility, e is the electronic charge, γ is a geometrical factor for ion hopping, λ is the hopping distance, k_B is the Boltzmann constant, and H_R is Haven's ratio. Equation 2 can be simplified to the following form:

$$\sigma_{dc} = KT^{-1}\omega_H \quad (3)$$

where K is the mobile concentration factor that depends upon the concentration of mobile ions and $\omega_H = 2\pi f_H$.[29]

Using eq 3, the mobile concentration factor, K, has been calculated for both $(PEO)_4$:$LiClO_4$ and $(PEO)_4$:$LiClO_4$ with 4 wt % δ-Al_2O_3. The values of K and its associated parameters σ_{dc} and f_h are shown at different temperatures for both samples in Table 1. On comparing the values corresponding to dc-conductivity, σ_{dc}, and hopping rate, f_h, for the polymer electrolytes, it is observed that the dc-conductivity and the hopping rate increase by approximately 2 orders of magnitude in the presence of δ-Al_2O_3 fillers, although a decrease in difference with increasing temperature is observed, as shown more clearly in Figure 3. It should also be noted that the K-value increased for electrolytes with fillers as compared to

dx.doi.org/10.1021/jp3036499 | J. Phys. Chem. B 2012, 116, 7762−7770

Table 1. Physical Parameters for $(PEO)_4$:$LiClO_4$:x wt % δ-Al_2O_3 (x = 0, 4)

	$(PEO)_4$:$LiClO_4$			$(PEO)_4$:$LiClO_4$:4 wt % δ-Al_2O_3		
temperature (K)	conductivity σ (S cm^{-1})	hopping freq f_H	conct factor K	conductivity σ (S cm^{-1})	hopping freq f_H	conct factor K
265	3.1×10^{-10}	2.9×10^{2}	4.5×10^{-11}	7.5×10^{-8}	5.1×10^{4}	6.1×10^{-11}
270	1.4×10^{-9}	1.0×10^{3}	5.6×10^{-11}	1.8×10^{-7}	1.2×10^{5}	6.4×10^{-11}
275	5.0×10^{-9}	3.7×10^{3}	5.8×10^{-11}	4.2×10^{-7}	2.7×10^{5}	6.7×10^{-11}
280	1.6×10^{-8}	9.9×10^{3}	7.0×10^{-11}	9.1×10^{-7}	5.2×10^{5}	7.8×10^{-11}

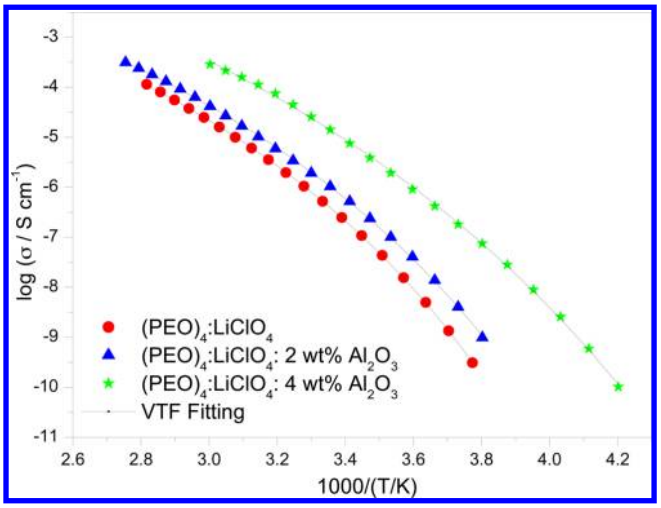

Figure 3. Temperature dependences of the dc-conductivities of $(PEO)_4$:$LiClO_4$:x wt % δ-Al_2O_3 (x = 0, 2, and 4).

without fillers, indicating an increase in mobile ion concentration in the presence of fillers. The fillers tend to improve the dissociation of the ion clusters and uncomplexed salt due to their active surface groups. The surface "−OH" group of the δ-Al_2O_3 fillers is expected to attract the ClO_4^- anions, thus weakening the association between $Li^+ClO_4^-$ ion pairs and increasing the free mobile Li^+ concentration.[30,31] However, it is evident from the data presented in Table 1 that the increase in conductivity in the presence of Al_2O_3 fillers can mainly be attributed to a greater hopping rate of the mobile Li^+ ions.

3.3. Temperature Dependence of the dc-Conductivity. The effect of δ-Al_2O_3 filler concentration on the dc-conductivity as a function of temperature is shown in Figure 3. The presence of 4 wt % δ-Al_2O_3 fillers increases the ionic conductivity from $\sigma_{dc} = 1.6 \times 10^{-7}$ S cm^{-1} to $\sigma_{dc} = 6.3 \times 10^{-6}$ S cm^{-1} at 298 K, and at lower temperatures, the enhancement in ionic conductivity is even more than 2 orders of magnitude. It can also be seen that all the samples exhibit a non-Arrhenius temperature dependence of the conductivity, which indicates that the ionic conductivity is mainly determined by the amorphous regions in the polymer electrolytes. This non-Arrhenius temperature dependence of the conductivity can be fitted by the Vogel−Tammann−Fulcher (VTF) equation, similar to the temperature dependence of the conductivity relaxation as discussed below in section 3.6.

3.4. Modulus Formalism. Analysis of impedance data in the modulus formalism has been used to analyze and interpret conductivity relaxation and ion dynamics, as it suppresses the electrode polarization effects occurring at low frequencies[32] and the modulus data can also be used for studying conductivity relaxation times.[33,34]

Parts a and b of Figure 4 show the frequency dependence of the imaginary part of the electric modulus, M'', for the compositions $(PEO)_4$:$LiClO_4$ and $(PEO)_4$:$LiClO_4$ with 4 wt %

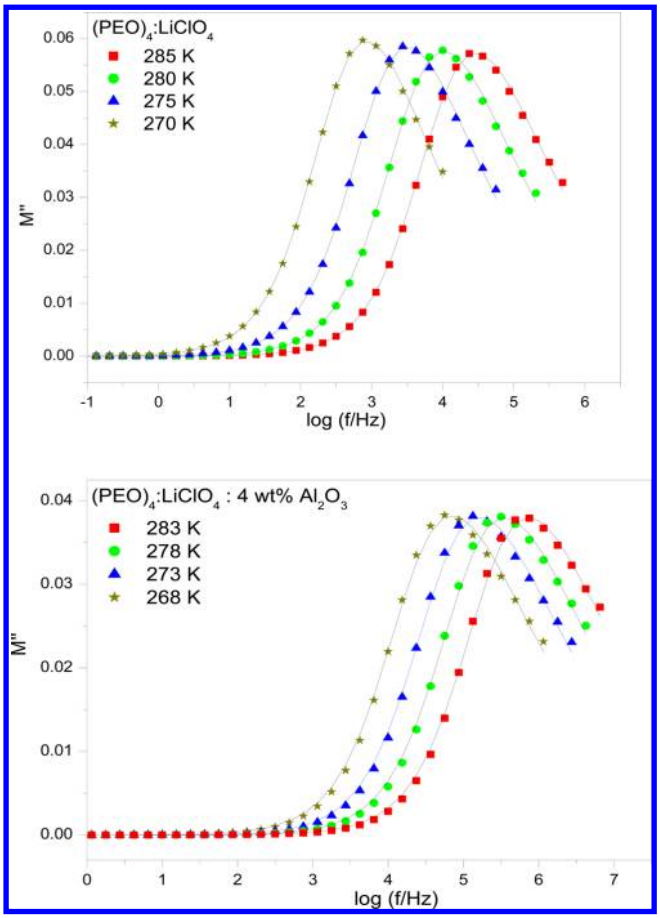

Figure 4. Variation of M'' as a function of frequency at different temperatures for (a) $(PEO)_4$:$LiClO_4$ and (b) $(PEO)_4$:$LiClO_4$ with 4 wt % δ-Al_2O_3. The solid lines represent fits to M'' by eq 6.

Al_2O_3, at different temperatures. The low value of M'' in the low frequency region indicates a negligible contribution of electrode polarization to the electric modulus. The peak in M'' is asymmetric and broader on both sides of the maxima than predicted by an ideal Debye behavior. It is also observed that the position of f_{max}, corresponding to M''_{max}, shifts toward higher frequencies with increasing temperature, for both polymer electrolytes. Furthermore, at a given temperature, f_{max} for the sample $(PEO)_4$:$LiClO_4$ with 4 wt % Al_2O_3 is observed to be higher than f_{max} for the sample without fillers. The frequency range below f_{max} suggests a range in which charge carriers are mobile over long distances, whereas on the high frequency side of f_{max} the charge carriers are confined to localized motions.[35] Thus, the peak frequency f_{max} is indicative of a transition from long-range to short-range mobility and it can also be considered as the frequency of the conductivity relaxation. The complex modulus can be expressed as the Fourier transform of the time derivative of the response function $\phi(t)$ given by

dx.doi.org/10.1021/jp3036499 | J. Phys. Chem. B 2012, 116, 7762−7770

$$M^*(\omega) = M_\infty\left[1 - \int_0^\infty \exp(-i\omega t)\left(\frac{d\phi(t)}{dt}\right)dt\right] \quad (4)$$

where $\phi(t)$ is defined by the empirical Kohlrausch–Williams–Watts (KWW) stretched exponential function[36]

$$\phi(t) = \exp[-(t/\tau)^\beta] \quad (5)$$

This function is suggestive of the asymmetric nature of M'' and describes the stretched exponential character of the relaxation of the electric field. τ is the characteristic relaxation time and β $(0 < \beta < 1)$ is the stretching parameter, which is 1 for a single exponential Debye-type relaxation and decreases with increasing stretching of the relaxation function, i.e., with an increasing deviation from a Debye-type relaxation.

The value of β can be determined by using the KWW function to fit the experimental data. However, since M'' is a function of frequency, it would be desirable to fit the data directly in the frequency domain, without needing to perform the Fourier transform. Fortunately, Bergman[37] has developed such a function in the frequency domain. The imaginary part of the electric modulus (M'') is then described as

$$M'' = \frac{M''_{max}}{(1-\beta) + (\beta/(1+\beta))[\beta(f_{max}/f) + (f/f_{max})^\beta]} \quad (6)$$

where M''_{max} is the peak value of M'' and f_{max} is the corresponding frequency. In the present case, the shape of each spectrum has been quantified by the β parameter obtained by fitting eq 6 to the experimental data, as shown in Figure 4a and b. The solid lines through the modulus spectra in Figure 4 show that the experimental data are well fitted by this model, except in the high frequency regime where other relaxation processes at higher frequencies may contribute. The values of β were found to be almost the same for all temperatures, within experimental errors. However, the value of the β parameter was found to decrease in the presence of fillers, suggesting a greater distribution of relaxation times.

The frequency dependent M'' of $(PEO)_4$:$LiClO_4$ and $(PEO)_4$:$LiClO_4$ with 4 wt % δ-Al_2O_3 have been scaled to produce single master curves, as observed in plots of M''/M''_{max} versus $\log(f/f_{max})$ shown in Figure 5. In general, such scaling studies have been performed in the literature to elucidate whether relaxation mechanisms are temperature independent or not.[38,39] We observe that, within experimental error, the M'' curves for all temperatures superpose onto one master curve. This suggests that the conductivity relaxation is a temperature independent dynamical process for each polymer electrolyte, i.e., both with and without Al_2O_3 nanofillers.

This leads to another important question: whether or not the modulus spectra, i.e., the M'' plots of polymer electrolytes with and without fillers, can be scaled to a common master plot. Figure 6 shows the superimposed M'' plots of both samples in the temperature range 270–285 K. From the figure, it is evident that the curves are not overlapping at the highest frequencies. This indicates that the presence of fillers tends to modify the local environment within the polymer electrolytes and thereby alter the conduction mechanism to some extent. MD simulations have suggested that a small fraction of the ether oxygen's of the PEO polymer chains tends to interact with filler particles.[40] However, this interaction is not attractive in nature, as the study suggests that a PEO chain does not completely curl around the filler particle but rather the same chain approaches and leaves the particle at a few points; i.e., the interaction between the polymer chains and the filler particles tends to alter the nature of the polymer chain packing around the filler particles and thereby alter the local environment within the polymer matrix, as compared to the polymer complex without fillers.

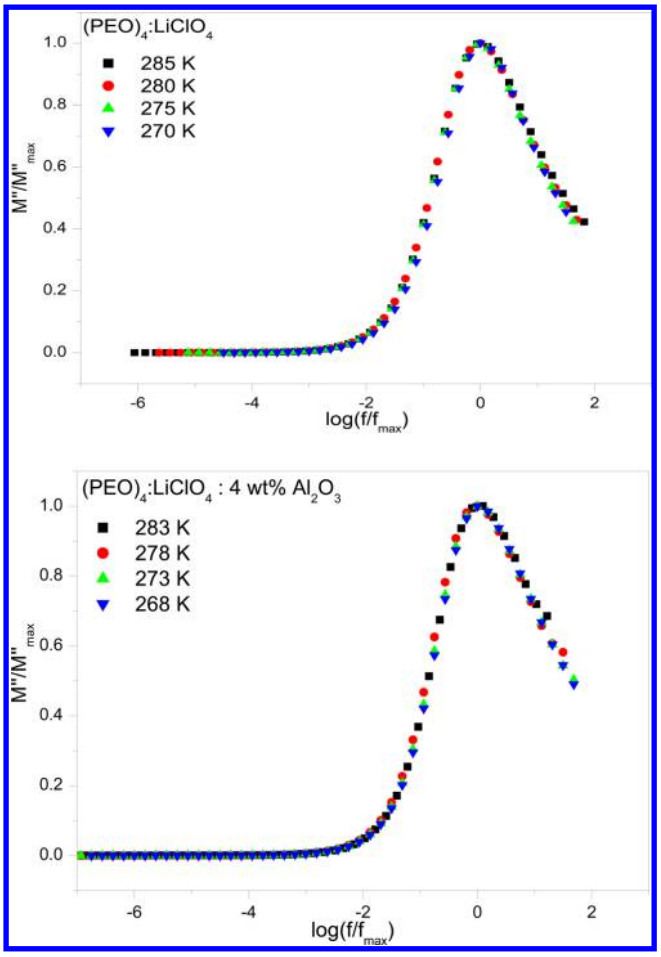

Figure 5. Plots of normalized (M''/M''_{max}) versus $\log(f/f_{max})$ for $(PEO)_4$:$LiClO_4$ and $(PEO)_4$:$LiClO_4$ with 4 wt % δ-Al_2O_3.

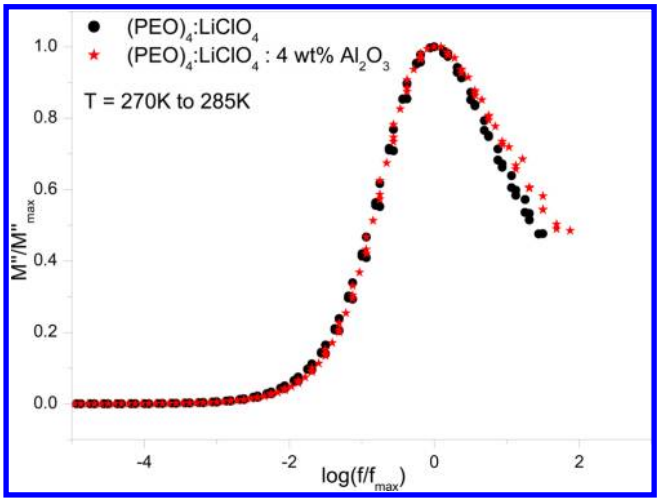

Figure 6. Superimposition of (M''/M''_{max}) versus $\log(f/f_{max})$ for $(PEO)_4$:$LiClO_4$ and $(PEO)_4$:$LiClO_4$ with 4 wt % δ-Al_2O_3 in a selected temperature range.

dx.doi.org/10.1021/jp3036499 | J. Phys. Chem. B 2012, 116, 7762–7770

3.5. Dielectric Relaxations. To account for the conductivity as well as relaxation processes in polymer electrolytes, the imaginary part of the dielectric permittivity (ε'') was analyzed using a sum of a conductivity term, a Havriliak–Negami function[41] for the α-process and Cole–Cole functions[42] for the β- and γ-processes. Thus, the total fitting function is given by eq 7:

$$\varepsilon''(\omega) = \frac{\sigma_{dc}}{\varepsilon_o \omega} + \frac{\Delta\varepsilon_\alpha}{(1 + (i\omega\tau_\alpha)^a)^b} + \frac{\Delta\varepsilon_\beta}{1 + (i\omega\tau_\beta)^a} + \frac{\Delta\varepsilon_\gamma}{1 + (i\omega\tau_\gamma)^a} \quad (7)$$

where $\omega = 2\pi f$ is the angular frequency, σ_{dc} is the dc-conductivity, and ε_o is the vacuum permittivity. The relaxation times and the dielectric strengths for the α-, β-, and γ-processes are represented as τ_α, τ_β, and τ_γ and $\Delta\varepsilon_\alpha$, $\Delta\varepsilon_\beta$, and $\Delta\varepsilon_\gamma$, respectively. The shape parameter "a" determines the symmetric broadening of the process, and the parameter "b" controls the asymmetric broadening.

The analysis of dielectric permittivity data provides important information to distinguish between dipolar relaxation processes (dielectric relaxation) and ionic conductivity processes in polymer electrolytes with and without nanofillers. Figure 7 shows the frequency dependence of the imaginary part

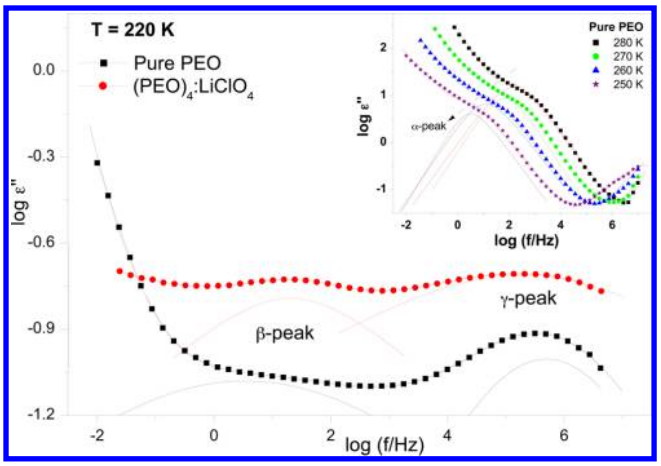

Figure 7. Dielectric loss (ε'') spectra of PEO and $(PEO)_4$:$LiClO_4$. Inset: The temperature dependence of the α-relaxation in pure PEO. The solid lines show fits to the α-, β-, and γ-relaxations.

of the permittivity, $\varepsilon''(\omega)$, for pure PEO and PEO with $LiClO_4$ at T = 220 K. The inset of Figure 7 shows $\varepsilon''(\omega)$ of pure PEO in the temperature range 250–280 K. The shoulder in these data is due to the primary structural α-relaxation, associated with segmental motions of the polymer chains. At the lowest frequencies, we observe that ε'' increases as $\sim\omega^{-1}$, which is the characteristic slope of pure ionic dc-conductivity, σ_{dc}.

In Figure 7, it can be seen that the secondary process, i.e., the β-relaxation is hardly observable for pure PEO. Since the β-relaxation can be associated with local segmental motions in amorphous regions confined between crystalline spherulite regions in PEO, the subtle signal of the β-relaxation suggests that these regions are limited in amount, as also supported from the high crystallinity (about 65%) of uncomplexed PEO. However, in the presence of the lithium salt, the β-relaxation becomes considerably stronger, and it can be observed as a distinguished peak. The dissolution of $LiClO_4$ in PEO increases the amorphous nature of the polymer electrolyte. The dissociated Li^+ ions tend to form coordinate bonds to the ether oxygens; i.e., the overall "free" length of the polymer chain is shortened due to the association with Li^+ ions. Thus, the most probable explanation for the increased intensity of the β-peak is the increase in the number of such "shortened" polymer chains exhibiting local segmental motions within the amorphous phase.[43,44]

In Figure 7, it can also be seen that the γ-relaxation, which most likely is due to a local twisting of chain ends as well as local intramolecular motions of the ethylene groups ($-CH_2-CH_2-$) in the polymer chains, becomes broader in the presence of $LiClO_4$. The reason for this is probably that the coordination of Li^+ ions to the ether oxygens affect this local relaxation by increasing the distribution of environments around the ethylene groups.

Figure 8 shows $\varepsilon''(\omega)$ of $(PEO)_4$:$LiClO_4$ and $(PEO)_4$:$LiClO_4$ with 2 and 4 wt % δ-Al_2O_3, respectively. It can be seen that the

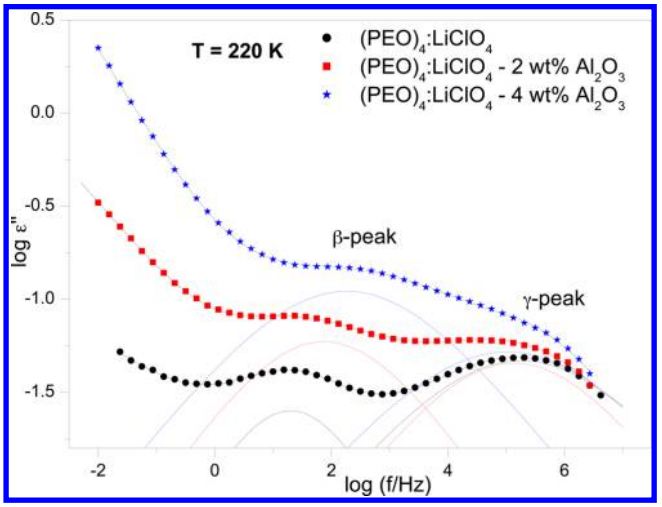

Figure 8. Dielectric loss spectra of $(PEO)_4$:$LiClO_4$:x wt % δ-Al_2O_3 (x = 0, 2, and 4). The solid lines show the fits to the β- and γ-relaxation peaks with Cole–Cole functions.

high frequency region of the spectra is dominated by the β- and γ-relaxation processes, whereas, at low frequencies, the increase in ε'' is associated with the high frequency wing of the α-relaxation, as well as a substantial contribution from the ionic conductivity, σ_{dc}, of the samples. Thus, also in this representation of the experimental data, it is evident that the polymer electrolyte with 4 wt % Al_2O_3 has the highest ionic conductivity. In the presence of the nanofillers, the polymer chains interact and anchor to filler particles at various ether oxygen atoms, i.e., the filler particles tend to "semibound" the polymer chains.[45] The intensity of the β-relaxation increases with increasing δ-Al_2O_3 concentration, and it also shifts to higher frequencies due to a speeding up of the relaxation process of these "semibounded" polymeric chains in the amorphous phase. However, the γ-relaxation seems to not be affected by the nanofillers, as it does not shift in frequency, change shape, or increase in peak intensity. In all the cases, except for pure PEO, the α-relaxation, corresponding to segmental motions of the polymer, is hidden in the strong conductivity contribution.

3.6. Temperature Dependences of the Relaxation Processes. The characteristic relaxation time, τ, of each relaxation process was obtained from the fitting of $\varepsilon''(\omega)$, as

dx.doi.org/10.1021/jp3036499 | J. Phys. Chem. B 2012, 116, 7762–7770

described above. The relaxation time corresponding to the dc-conductivity loss was estimated from the reciprocal of the frequency corresponding to the peak maximum of the imaginary part of the modulus $M''(\omega)$. In order to understand how the fillers affect the dynamic relaxation processes of the pure polymer, the dielectric spectra of pure PEO and PEO with 4 wt % Al_2O_3 fillers were analyzed. Figure 9 shows the

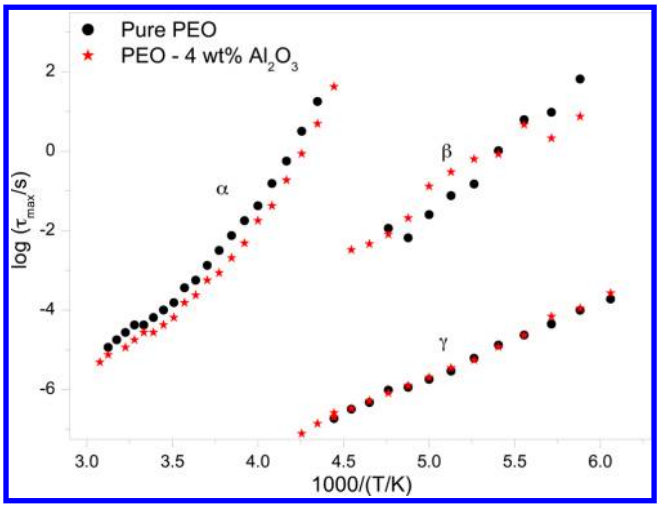

Figure 9. Temperature dependences of the α-, β-, and γ-relaxation times in PEO and PEO with 4 wt % δ-Al_2O_3.

temperature dependences of the α-, β-, and γ-relaxation times in PEO and PEO with fillers. The α-relaxation of both samples shows a non-Arrhenius temperature dependence, and the nanofillers give rise to a speeding up of this relaxation process. As mentioned above, MD simulations and DSC studies have indicated that the interactions between the polymer chains and the filler particles are nonattractive, such that the PEO polymer chains just tend to "curl" around the nanofillers but without being strongly adsorbed on the filler particle. Such interactions between polymer chains and filler particles tend to increase the "free volume" around these polymer chains as well as distort the local polymer environment. These structural alterations, with increased "free volume", may be the reason for the increased relaxation rate of the segmental polymer dynamics, i.e., the α-relaxation, in the presence of δ-Al_2O_3 nanofillers. The β- and γ-relaxation times, on the other hand, show Arrhenius temperature dependences, and they are not much affected by the nanofillers, as can be seen in Figure 9.

Figure 10 shows the temperature dependences of the conductivity and β- and γ-relaxation times of $(PEO)_4$:$LiClO_4$ with and without δ-Al_2O_3 fillers. The non-Arrhenius temperature dependence of the conductivity relaxation indicates that the conduction process is of cooperative character, in contrast to the noncooperative β- and γ-relaxations with Arrhenius temperature dependences. Both the conductivity relaxation and the β-relaxation become faster with increasing filler concentration, whereas the γ-relaxation time seems to be unaffected by the lithium salt and the nanofillers. The conductivity relaxation shows a VTF behavior, as expected from the temperature dependence of the dc-conductivity shown in Figure 3.

The VTF equation may be used to describe the temperature dependence of the conductivity relaxation.[46]

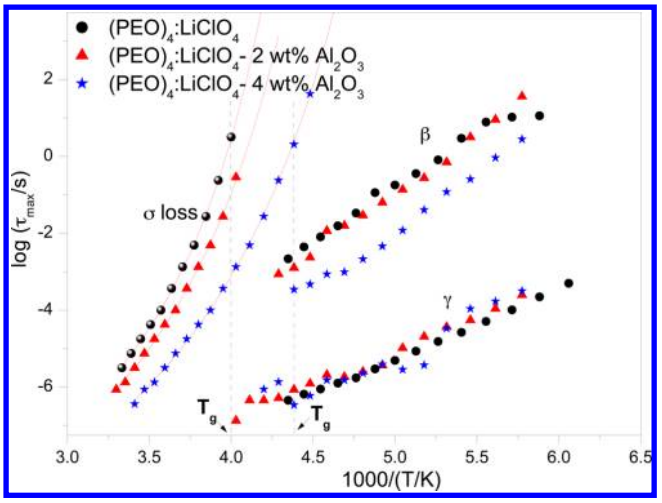

Figure 10. Temperature dependences of the conduction loss and the β and γ relaxation times of $(PEO)_4$:$LiClO_4$:x wt % δ-Al_2O_3 (x = 0, 2, and 4). The solid curves shows fits by the VFT equation.

$$\tau_\sigma = \tau_o \exp\left(\frac{DT_o}{T - T_o}\right) \quad (8)$$

where τ_o is the pre-exponential factor and T_0 a reference temperature equivalent to the Kauzmann temperature.[47] The "strength parameter" D is related to the "strong" and "fragile" classification, determined by the change in dynamic properties, such as viscosity, structural relaxation time, and diffusion constant, of amorphous systems above T_g.[46,48] The structural (α) relaxation of strong systems follows a nearly Arrhenius temperature dependence,[46,49] whereas fragile systems exhibit a pronounced departure from the Arrhenius law.[50]

The "D" values for $(PEO)_4$:$LiClO_4$ with 0, 2, and 4 wt % Al_2O_3 are found to be around 6.6, 8.4, and 9.6, respectively. The increase in the D value indicates that the presence of fillers decreases the fragility of the polymer electrolyte system.[51] Thus, from thermal characterization and conductivity studies, we observe decreases in glass transition temperature and fragility in the presence of Al_2O_3 fillers, which indicate that the polymer–filler interaction is nonattractive. This finding is fully consistent with a recent simulation study by Starr and Douglas,[52] where they showed that both T_g and fragility decrease when the polymer–filler interaction is nonattractive.

In Figure 10, it is also evident that the conductivity relaxation time is approximately 10 s at the calorimetric glass transition temperature T_g, both with and without filler particles. Since T_g, by definition, corresponds to the temperature where the structural α-relaxation process reaches a time scale of about 100 s, this implies that the ionic conduction process "freezes in" on this time scale at about the same temperature as the α-relaxation "freezes in". Thus, even if the dielectric studies show that the α-relaxation is hidden in the strong contribution from conductivity and therefore could not be directly observed, all the experimental data presented in this paper strongly suggest that the conductivity relaxation and the dc-conductivity are directly coupled to the hidden α-relaxation, even in the presence of nanofillers (at least in the case of δ-Al_2O_3 nanofiller concentrations up to 4 wt %). Furthermore, the polymer chains near the "interactive" surface of nanoparticles experience an increase in mobility when they are repelled by the nanoparticles, due to an increased "free volume" in this region. Simulations have suggested that the "polymer sphere" formed

dx.doi.org/10.1021/jp3036499 | J. Phys. Chem. B 2012, 116, 7762–7770

around filler particles tends to expel most of the Li^+ ions away from the surface of the filler particles into the polymer surroundings, with the consequence that only a few free Li^+ ions will reside between the filler particles and the surrounding polymer chains.[40] With the increased "free volume" and the altered local environment of the Li^+ ions, the segmental motions of the polymer chains speed up, i.e., the relaxation time of the viscosity related structural (α) relaxation decreases, and thereby facilitate a faster migration of the Li^+ ions. According to Wieczorek et al.,[53,54] Lewis acid−base type surface groups on alumina grains interact with cations and provide additional sites, creating favorable high conducting pathways for the migrating ions in the vicinity of the grains. Another proposed explanation is given by considering the surface activity of the filler particles and the creation of static surface pathways for ionic motions by decoupling the diffusion of ions from the relaxation of the polymer chains.[10,55] Although we cannot exclude that such conduction mechanisms are present in the here studied samples containing nanofillers, it is important to note that our observed speeding up the segmental polymer dynamics, and the associated decrease in T_g, is sufficient to explain the nanofiller induced enhancement of the ionic conductivity for low concentrations of δ-Al_2O_3 nanofillers.

4. CONCLUSIONS

The present investigation mainly focused on the effect of δ-Al_2O_3 nanofillers on the glass transition temperature and dielectric relaxations in the polymer electrolyte $(PEO)_4$:$LiClO_4$. The thermal studies of the polymer electrolytes show that the glass transition temperature tends to decrease with increasing δ-Al_2O_3 filler content, indicating that the segmental polymer dynamics speeds up with increasing filler concentration, at least at temperatures around the glass transition temperature.

The dielectric conductivity studies show that the ionic dc-conductivity of the polymer electrolyte enhances by approximately 2 orders of magnitude with the addition of 4 wt % δ-Al_2O_3. By combining these conductivity data with the DSC data, we are able to reach the important conclusion that the increase in ionic conductivity with increasing concentration of filler particles can be explained by a speeding up of the segmental polymer dynamics, i.e., the viscosity related α-relaxation. Hence, the combined data indicates a direct coupling between Li^+ ion motions and polymer segmental dynamics (at least in the case of δ-Al_2O_3 nanofillers of concentrations up to 4 wt %). Furthermore, it was observed that the temperature dependence of the conductivity exhibits a non-Arrhenius behavior, which suggests that the amorphous regions in the polymer electrolytes determine the ionic conductivity. We also found that the fragility of the polymer electrolyte decreases with increasing filler concentration. From the decrease in T_g and fragility, it can be concluded that the interaction between the nanofillers and the polymer is mainly nonattractive in nature. This nonattractive interaction between polymer chain segments and filler particles tends to alter the conformation of the polymer chains in the vicinity of the filler particles and thereby alter the local environment within the polymer matrix, as compared to the polymer complex without fillers.

It was also observed that the modulus (M'') plots of the polymer electrolytes with and without fillers could not be scaled to a common master plot at higher frequencies. This further supports that the presence of fillers causes alterations of the local environment within the polymer.

The dielectric relaxation studies of $(PEO)_4$:$LiClO_4$ with and without δ-Al_2O_3 show that there are three distinct dielectric relaxation processes, α, β, and γ, in the systems. While the α-relaxation cannot be directly observed due to a strong conductivity contribution, the β-relaxation process of the polymer becomes stronger and also shifts to higher frequencies due to a speeding up of the relaxation process of the "semibounded" polymeric chains in the amorphous phase. In contrast, the γ-relaxation, associated with the local twisting of chain ends as well as local intramolecular motions of the ethylene groups ($-CH_2-CH_2$) in the polymer chains, seems to not be affected by the nanofillers, as it does not shift in frequency, change shape, or increase in peak intensity.

AUTHOR INFORMATION

Corresponding Author

*E-mail: moneyb@chalmers.se.

Notes

The authors declare no competing financial interest.

ACKNOWLEDGMENTS

The authors wish to acknowledge the Swedish Research Council Formas and the Swedish Energy Agency for financial support.

REFERENCES

(1) Song, J. Y.; Wang, Y. Y.; Wan, C. C. *J. Power Sources* **1999**, *77*, 183−197.
(2) Wintersgill, M. C.; Fontanella, J. J. *Polymer Electrolyte Reviews 2*; MacCallum, J. R., Vincent, C. A., Eds.; Elsevier: London, New York, 1989; p 43.
(3) Quartarone, E.; Mustarelli, P; Magistris, A. *Solid State Ionics* **1998**, *110*, 1−14.
(4) Croce, F.; Appetecchi, G. B.; Persi, L.; Scrosati, B. *Nature* **1998**, *394*, 456−458.
(5) Zhou, J; Fedkiw, P. S. *Solid State Ionics* **2004**, *166*, 275−293.
(6) Gu, H.; Huang, Y.; Zhang, X.; Wang, Q.; Zhu, J.; Shao, L.; Haldolaarachchige, N.; Young, D. P.; Wei, S; Guo, Z. *Polymer* **2012**, *53*, 801−809.
(7) Wei, H.; Yan, X.; Li, Y.; Wu, S.; Wang, A.; Wei, S.; Guo, Z. *J. Phys. Chem. C* **2012**, *116*, 4500−4510.
(8) Krawiec, W.; Scanlon, L. G., Jr.; Fellner, J. P.; Vaia, R. A.; Vasudevan, S.; Giannelis, E. P. *J. Power Sources* **1995**, *54*, 310−315.
(9) Sun, H. Y.; Sohn, H.-J.; Yamamoto, O.; Takeda, Y.; Imamishi, N. *J. Electrochem. Soc.* **1999**, *146*, 1672−1676.
(10) Jayathilaka, P. A. R. D.; Dissanayake, M. A. K. L.; Albinsson, I.; Mellander, B. E. *Electrochim. Acta* **2002**, *47*, 3257−3268.
(11) Croce, F.; Persi, L.; Scrosati, B.; Serraino-Fiory, F.; Plichta, E.; Hendrickson, M. A. *Electrochim. Acta* **2001**, *46*, 2457−2461.
(12) Porter, C. H.; Boyd, R. H. *Macromolecules* **1971**, *4*, 589−594.
(13) Connor, T. M.; Read, B. E.; Williams, G. *J. Appl. Chem.* **1964**, *14*, 74−81.
(14) Ishida, Y.; Matsuo, M.; Takayanagi, M. *J. Polym. Sci., Part B* **1965**, *3*, 321−324.
(15) Heaton, N. J.; Benavente, R.; Pérez, E.; Bello, A.; Pereña, J. M. *Polymer* **1996**, *37*, 3791−3798.
(16) Ferloni, P.; Chiodelli, G.; Magistris, A.; Sanesi, M. *Solid State Ionics* **1986**, *18&19*, 265−270.
(17) Nasir, N. H. A.; Chan, C. H.; Kammer, H. W.; Sim, L. H.; Yahya, M. Z. A. *Macromol. Symp.* **2010**, *290*, 46−55.
(18) Choi, B.-K.; Kim, Y.-W.; Shin, K.-H. *J. Power Sources* **1997**, *68*, 357−360.
(19) Syzdek, J. S.; Armand, M. B.; Falkowski, P.; Gizowska, M.; Karłowicz, M.; Łukaszuk, Ł.; Marcinek, M. Ł.; Zalewska, A.; Szafran, M.; Masquelier, C.; et al. *Chem. Mater.* **2011**, *23*, 1785−1797.

(20) Ferloni, P.; Chiodelli, G.; Magistris, A.; Sanesi, M. *Solid State Ionics* **1986**, *18 and 19*, 265−270.
(21) Robitaille, C. D.; Fauteux, D. J. *J. Electrochem. Soc.* **1986**, *133*, 315−325.
(22) Bansal, A.; Yang, H.; Li, C.; Cho, K.; Benicewicz, B. C.; Kumar, S. K.; Schadler, L. S. *Nat. Mater.* **2005**, *4*, 693−698.
(23) Starr, F. W.; Schrøder, T. B.; Glotzer, S. C. *Phys. Rev. E* **2001**, *64* (021802), 1−5.
(24) Torres, J. A; Nealey, P. F.; de Pablo, J. J. *Phys. Rev. Lett.* **2000**, *85*, 3221−3224.
(25) Almond, D. P.; West, A. R. *Solid State Ionics* **1983**, *11*, 57−64.
(26) Ahmad, M. M. *Phys. Rev. B* **2005**, *72* (174303), 1−4.
(27) Dutta, D.; Ghosh, A. *Phys. Rev. B* **2005**, *72* (024201), 1−6.
(28) Bhattacharya, S.; Ghosh, A. *Phys. Rev. B* **2006**, *74* (184308), 1−5.
(29) El-Egili, K. *J. Phys.: Condens. Matter* **1996**, *8*, 3419−3426.
(30) Singh, T. J.; Bhat, S. V. *J. Power Sources* **2004**, *129*, 280−287.
(31) Wang, Z; Hu, Y; Chen, L. *J. Power Sources* **2005**, *146*, 51−57.
(32) Hodge, I. M.; Ingram, M. D.; West, A. R. *J. Electroanal. Chem.* **1976**, *74*, 125−143.
(33) Reau, J. M.; Jun, X. Y.; Senegas, J.; Le Deit, Ch.; Poulain, M. *Solid State Ionics* **1997**, *95*, 191−197.
(34) Ghosh, S.; Ghosh, A. *Solid State Ionics* **2002**, *149*, 67−72.
(35) Bobe, J. M.; Reau, J. M.; Senegas, J.; Poulain, M. *Solid State Ionics* **1995**, *82*, 39−52.
(36) Williams, G.; Watts, D. C. *Trans. Faraday Soc.* **1970**, *66*, 80−85.
(37) Bergman, R. *J. Appl. Phys.* **2000**, *88* (1356), 1−10.
(38) Ghosh, A.; Pan, A. *Phys. Rev. Lett.* **2000**, *84*, 2188−2190.
(39) Sidebottom, D. L. *Rev. Mod. Phys.* **2009**, *81*, 999−1014.
(40) Kasemägi, H.; Klintenberg, M.; Aabloo, A.; Thomas, J. O. *J. Mater. Chem.* **2001**, *11*, 3191−3196.
(41) Havriliak, S.; Negami, S. *Polymers* **1967**, *8*, 161−210.
(42) Cole, K. S.; Cole, R. H. *J. Chem. Phys.* **1941**, *9*, 341−351.
(43) Lorthioir, C.; Alegria, A.; Colmenero, J.; Deloche, B. *Macromolecules* **2004**, *37*, 7808−7817.
(44) Napolitano, S.; Wübbenhorst, W *J. Non-Cryst. Solids* **2007**, *353*, 4357−4361.
(45) Fragiadakis, D.; Pissis, P. *J. Non-Cryst. Solids* **2007**, *353*, 4344−4352.
(46) Angell, C. A. *J. Non-Cryst. Solids* **1991**, *131−133*, 13−31.
(47) Kauzmann, W. *Chem. Rev.* **1948**, *43*, 219−256.
(48) Hodge, I. M. *J. Non-Cryst. Solids* **1996**, *202*, 164−172.
(49) Borde, B.; Bizot, H.; Vigier, G.; Buleon, A *Carbohydr. Polym.* **2002**, *48*, 83−96.
(50) Kaushal, A. M.; Bansal, A. K. *Eur. J. Pharm. Biopharm.* **2008**, *69*, 1067−1076.
(51) Agapov, A. L.; Sokolov, A. P. *Macromolecules* **2011**, *44*, 4410−4414.
(52) Starr, F. W.; Douglas, J. F. *Phys. Rev. Lett.* **2011**, *106* (115702), 1−4.
(53) Marcinek, M.; Bac, A.; Lipka, P.; Zaleska, A.; Zukowska, G.; Borkowska, R.; Wieczorek, W. *J. Phys. Chem. B* **2000**, *104*, 11088−11093.
(54) Wieczorek, W.; Florjanczyk, Z.; Stevens, J. R. *Electrochim. Acta* **1995**, *40*, 2251−2258.
(55) Tambelli, C. C.; Bloise, A. C.; Rosário, A. V.; Pereira, E. C.; Magon, C. J.; Donoso, J. P. *Electrochim. Acta* **2002**, *47*, 1677−1682.